



27 <sup>13</sup>Institute of Forest Ecology SAS, Zvolen, Slovakia

28 <sup>14</sup>School of Agricultural, Forest and Food Sciences HAFL, Bern University of Applied  
29 Sciences, Zollikofen, Switzerland

30 <sup>15</sup> University of Toulouse, INRAE, UMR DYNAFOR, Castanet-Tolosan, France

31 <sup>16</sup>CNPF-CRPF Occitanie, Tarbes, France

32 <sup>17</sup>Forest Dynamics, Swiss Federal Research Institute WSL, Birmensdorf, Switzerland

33 <sup>18</sup>Institute of Terrestrial Ecosystems, ETH Zurich, Universitätstrasse 16, 8092 Zurich,  
34 Switzerland

35 <sup>19</sup>Ecology group, Department Biology, University of Erlangen-Nuremberg, Erlangen,  
36 Germany

37 <sup>20</sup>Ecosystem Dynamics and Forest Management, Technical University of Munich, Freising,  
38 Germany

39 <sup>21</sup>Berchtesgaden National Park, Berchtesgaden, Germany

40 <sup>22</sup>Research Institute for Nature and Forest INBO, Geraardsbergen, Belgium

41

42 \*Corresponding author:

43 Jan Christian Habel, Evolutionary Zoology, Department of Biosciences, University of  
44 Salzburg, Hellbrunner Str. 34, AT-5020 Salzburg, Austria; Mail: Janchristian.habel@sbg.ac.at

45

46 Running title: Biogeography of *Bolitophagus reticulatus*

47

48 **ABSTRACT**

49 The geographic distributions of species associated with European temperate broadleaf forests  
50 were significantly influenced by glacial-interglacial cycles. These species persisted the glacial  
51 periods in Mediterranean and extra-Mediterranean refugia and expanded northwards during  
52 the interglacial stages. The common saproxylic beetle *Bolitophagus reticulatus* closely  
53 depends on European temperate broadleaf forests. The beetle mostly develops in the tinder  
54 fungus *Fomes fomentarius*, a major decomposer of broadleaf-wood. We sampled *B.*  
55 *reticulatus* in sporocarps from European (*Fagus sylvatica*) and Oriental beech (*F. orientalis*)  
56 across Europe and the Caucasus region. We analysed mitochondrial gene sequences (*cox1*,  
57 *cox2*, *cob*) and microsatellites to reconstruct the geographic distribution of glacial refugia and  
58 postglacial recolonization pathways. We found only marginal genetic differentiation of *B.*  
59 *reticulatus*, except for a significant split between populations of the Caucasus region and  
60 Europe. This indicates the existence of past refugia south of the Great Caucasus, and a contact  
61 zone with European populations at the Crimea region. Further, potential refugia might have  
62 been located at the foothills of the Pyrenees and the Balkan region. Our genetic data suggest a  
63 phalanx-wise recolonization of Europe, which reflects the high mobility of this beetle species.

64

65 Keywords: Broadleaf forest, *Fomes fomentarius*, biogeography, genetic analysis, refugia,  
66 expansion, phalanx-wise, mobility

67

68 **INTRODUCTION**

69 The glacial-interglacial cycles of the Pleistocene caused severe range shifts of most species  
70 across Europe (Hewitt, 1999; 2000; Schmitt, 2007; Schmitt & Varga, 2012). Many European  
71 species persisted the past glacial periods in Mediterranean refugia (Hewitt, 1999), as well as  
72 in extra-Mediterranean refugia of Central Europe (Schmitt & Varga, 2012). Also the ponto-  
73 caspian area was proposed as potential glacial refugium for European taxa (Tarkhnishvili *et*  
74 *al.*, 2012, Neiber & Hausdorf, 2015). These range modifications resulted in inter- and  
75 intraspecific genetic signatures, such as differentiation through long-term isolation in disjunct  
76 glacial refugia (Hewitt, 2000). Also range expansions after glacial periods are reflected in the  
77 genetics of species. They follow two propagation patterns: a pioneer process (with the two  
78 types, stepping stone wise and leptokurtic), implying repeated founder effects in the wake of  
79 population expansions into new habitat patches (Ibrahim *et al.*, 1996). This propagation  
80 pattern creates typical signatures of gradual loss of genetic diversity in the course of  
81 colonization (Ibrahim *et al.* 1996). In contrast, phalanx-wise colonization implies area-wide  
82 expansion, and therefore a lack of genetic signatures along colonization routes (Hewitt, 2000).

83  
84 The biogeography of broadleaf tree species has been intensively studied during the past years  
85 (Pott, 2000; Brunet *et al.*, 2010). Forests dominated by broadleaves currently occur in diverse  
86 ecoregions and include the Atlantic, Central European, Balkan, Baltic, Dinaric, and Caucasus  
87 mixed forests, which are equipped with typical plant, fungus, and animal species (Brunet *et*  
88 *al.*, 2010; Müller *et al.*, 2013). They have persisted in disjunct glacial refugia. Tree species  
89 with high cold tolerances, such as birch (*Betula* sp.), occurred in extra-Mediterranean and  
90 northern refugia during the glacial stages (Svenning, *et al.*, 2008; Giesecke *et al.*, 2017). More  
91 thermophilic tree species, such as European beech (*Fagus sylvatica*), persisted the glacial  
92 stages in various disjunct Mediterranean refugia, as well as in a number of cryptic extra-  
93 Mediterranean refugia along the edge of the Eastern Alps, the Balkan Peninsula and northern

94 Spain (Magri *et al.*, 2006, 2008; Saltré *et al.*, 2013). After the last glacial period, the European  
95 beech recolonized central and northern Europe mainly from the Balkan region (Magri *et al.*,  
96 2006), while the populations in the western Mediterranean area, such as northern Spain,  
97 played a rather minor role as potential sources for recolonization (Magri *et al.*, 2006, 2008;  
98 Saltré *et al.*, 2013).

99

100 While the biogeographic history of all tree species forming the European broadleaf forests is  
101 well studied (Magri *et al.*, 2006, 2008; Svenning, *et al.*, 2008; Saltré *et al.*, 2013; Giesecke *et*  
102 *al.*, 2017), comparably little data and evidence on the biogeographic history of animal species  
103 relying on European broadleaf forests are available (Stauffer *et al.*, 1999; Rukke, 2000; Pons  
104 *et al.*, 2011; Drag *et al.*, 2011, 2015, 2018; Jiménez-Alfaro *et al.*, 2018). Moreover, in many  
105 of these studies the Caucasus region is not considered, although further refugia could have  
106 been located in this region.

107

108 In this study we analysed the genetic structure of the darkling beetle *Bolitophagus reticulatus*  
109 (Linnaeus, 1767) (Tenebrionidae, Tenebrionini, Bolitophagini), a typical representative of the  
110 fauna of European broadleaf forest. The larvae and adults live in polypores and mostly inhabit  
111 the tinder fungus *Fomes fomentarius* (L.) Fr. 1849 (Midtgaard *et al.*, 1998, 2013; Nilsson,  
112 1997). The beetle species is widespread across the Palaearctic region and very mobile  
113 (Jonsson, 2003). We sampled individuals of this species across its Western Palaearctic  
114 distribution range, including the Caucasus region. We analysed mitochondrial DNA  
115 sequences and polymorphic microsatellites allowing the investigation at different rates of  
116 evolution. Based on these data we identify past glacial refugia and range expansions during  
117 interglacial periods. In particular we aim to answer the following questions:

- 118 1. Do the refugial areas of *B. reticulatus* correspond to the refugia of tree species being  
119 part of the European broadleaf forest?

- 120 2. What is the role of the Caucasian region in the context of glacial survival and  
121 postglacial recolonization of the Western Palearctic?
- 122 3. How did post-glacial range expansion take place, pioneer- or phalanx-wise?
- 123 4. Do genetic structures coincide with the ecology and behaviour of *B. reticulatus*?
- 124

## 125 MATERIAL AND METHODS

### 126 Study species

127 The genus *Bolitophagus* is represented in the Palearctic by a total of four species (Iwan *et al.*,  
128 2020). The most widespread species is *Bolitophagus reticulatus*, having a Palearctic  
129 distribution, but being absent from the central Mediterranean. Its larvae and adults live in  
130 polypores and are among the most frequent inhabitants of the tinder fungus *Fomes*  
131 *fomentarius* (Friess *et al.*, 2019). Adults of the beetle feed on spores from living basidiocarps,  
132 but are also commonly found in dead and deteriorated polypores, where its larvae develop  
133 (Midtgaard *et al.*, 1998, 2013). Experimental studies found single individuals to fly up to  
134 125 km in a flight mill experiment (Jonsson, 2003). This high mobility is also supported by  
135 local scale studies (Jonsson *et al.*, 2003; Zytynska *et al.*, 2018). The main host of *B.*  
136 *reticulatus* is *F. fomentarius* (Nilsson, 1997), but it was also recorded from other polypores  
137 (e.g. *Phellinus nigricans*, *Fomitopsis pinicola*, *Piptoporus betulinus*, *Ganoderma applanatum*,  
138 *Laetiporus sulphureus* and *Daedaleopsis* spp.; Bouget *et al.*, 2019). *F. fomentarius* occurs on  
139 a range of broadleaf tree species, mostly beech (*Fagus* spp.) and birch (*Betula* spp.), but rarely  
140 also others like oak (*Quercus* spp.) and maple (*Acer* spp.).

141

### 142 Sampling

143 We collected 281 individuals of *B. reticulatus* from 57 beech forest sites across major parts of  
144 the beetle's western Palaeartic distribution range, including the Caucasus region. We  
145 sampled five individuals at each site (wherever possible). Sampling was conducted during the  
146 years 2014, 2015, and 2017. We extracted the individuals from sporocarps of *F. fomentarius*  
147 and subsequently stored them in 99% ethanol until further analyses. An overview of all  
148 sampling sites including GPS coordinates is compiled in Appendix Table S1. All individuals  
149 used in this study are stored at the Terrestrial Ecology Research Group, Technical University  
150 Munich (TUM), Freising, Germany.

151

## 152 **Molecular analyses**

153 DNA was extracted from head, thorax and fore legs applying the Qiagen DNeasy kit (Qiagen,  
154 Hilden, Germany) based on the standard protocol for tissue samples. Partial mitochondrial  
155 genes cytochrome oxidase subunit I (*cox1*), cytochrome c oxidase subunit II (*cox2*), and  
156 cytochrome b (*cob*) were amplified using the primer combinations and PCR conditions  
157 described in Rangel López *et al.* (2018). Successfully amplified PCR products were purified  
158 with ExoSap (Thermo Fischer Scientific) and subsequently sequenced in both directions by  
159 the Genomics Service Unit (GSU) of the Ludwig-Maximilians-Universität München (LMU),  
160 Germany. We successfully generated *cox1*, *cox2*, and *cob* sequences for 208 individuals (out  
161 of the 281 individuals sampled). An overview of all sequences and GenBank accession  
162 numbers are given in Appendix Table S2.

163

164 We successfully genotyped seventeen polymorphic microsatellites for 255 individuals (out of  
165 the 281 individuals sampled) (Appendix Table S2), with the same primers and conditions  
166 successfully applied in a previous study (Zytynska *et al.*, 2018). We used two multiplex  
167 combinations, each with 8-9 primer pairs, using three fluorescent dyes: 6-FAM, HEX, and  
168 TAMRA, alongside the ROX size standard. PCR products were run on an ABI 3130xl Genetic  
169 Analyzer (Applied Biosystems – Life Technologies GmbH, Darmstadt, Germany) at the GSU  
170 of the LMU, Germany. Further details on protocols applied are given in Zytynska *et al.*  
171 (2018).

172

## 173 **Phylogenetic and demographic analyses**

174 Forward and reverse reads of mtDNA sequences were assembled with GENEIOUS v. 6.1.8  
175 (<https://www.geneious.com>). After removing primer sequences and low-quality base calls



176 from the sequence ends, multiple sequence alignment was performed per marker using the  
177 MUSCLE (Edgar, 2004 a, b) algorithm as implemented in GENEIOUS.

178

179 Mitochondrial haplotypes were extracted from the aligned mitochondrial supermatrix in  
180 PEGAS v. 0.13 (Paradis, 2010). Individuals with more than 100 missing sites were excluded  
181 and sites with missing or ambiguous data were disregarded. Haplotype networks were inferred  
182 using an infinite sites model (i.e. uncorrected distance) with PEGAS and the spatial distribution  
183 of haplotypes was mapped with a combination of the *R*-packages MAPS v. 3.3.0 (Becker *et al.*,  
184 2018), RASTER v. 3.1-5 (Hijmans, 2020), and GGLOT2 v. 3.3.0 (Wickham, 2016).

185

186 A phylogenetic tree was inferred with IQ-TREE v. 2.0-rc2 (Minh *et al.*, 2020). *Nalassus*  
187 *laevioctostriatus*, *Opatrum sabulosum*, and *Eledonoprius armatus* were chosen as outgroup  
188 based on an already published phylogeny of tenebrionid beetles (Kergoat *et al.*, 2014).  
189 Respective sequences were obtained from NCBI GenBank (Appendix Table S2). Data was  
190 partitioned into the three genes (*cox1*, *cox2*, *cob*) and their codon positions for a total of 9  
191 initial partitions used as input for MODELFINDER (Kalyaanamoorthy *et al.*, 2017). This  
192 approach not only selects the best fitting substitution model for each partition, but also merges  
193 initial partitions according to their statistical properties to reduce parameter space. The top ten  
194 percent of partition pairs were evaluated (option *-rcluster 10*). The heuristic tree search was  
195 repeated 10 times. The best tree was chosen and rooted with *Opatrum sabulosum*.  $1 \times 10^5$   
196 ultrafast bootstrap replicates were performed to provide branch support (Hoang *et al.*, 2018).

197

198 We performed Coalescent Bayesian Skyline analysis (Drummond *et al.*, 2005) with BEAST  
199 v. 2.6.2 (Boukaert *et al.*, 2014). Outgroups were excluded for this analysis. An estimate of the  
200 *cox1* substitution rate in tenebrionid beetles ( $3.54 \pm 0.38 \% \text{ My}^{-1}$ ) (Papadopoulou *et al.*, 2010)  
201 was used to calibrate the mitochondrial tree in time, using the mean estimate with a relaxed

202 lognormal molecular clock model. Optimal models of nucleotide substitution and partition  
203 scheme were inferred with MODELFINDER (Kalyaanamoorthy *et al.*, 2017) in IQ-TREE; initial  
204 partitions were set to the three genes. The topology was linked across genes. Three  
205 independent MCMCs were run for  $8 \times 10^7$  generations, with sampling every  $5 \times 10^3$  generations.  
206 Convergence of independent runs to similar values, stationarity, and effective sample sizes  
207 were assessed in TRACER v. 1.7.1 (Rambaut *et al.*, 2018) after removing a burn-in of 25 % of  
208 samples. Based on the combined post-burn-in sample of all three runs, Bayesian Skyline plots  
209 were generated with TRACER and *ggplot2* v. 3.3.0 (Wickham, 2016). The posterior sample of  
210 trees was summarized with TREEANNOTATOR from the BEAST software package, using  
211 maximum clade credibility and common ancestor heights.

212

### 213 **Analyses of population structure**

214 Analyses of population structure were done with microsatellite data using R v. 4.0.2 (R Core  
215 Team, 2019) in R-STUDIO v. 1.2.1335 (RStudio Team, 2018). Mean  $F_{ST}$ ,  $G_{ST}$ ,  $G'_{ST}$ , and  $D_{Jost}$   
216 were calculated as basic descriptive molecular statistics of population differentiation per  
217 locus. Allelic richness and number of unique allele combinations, as well as mean observed  
218 and mean expected heterozygosity were calculated using the packages POPPR v. 2.8.5  
219 (Kamvar *et al.*, 2014; 2015), DIVERSITY v. 1.9.90 (Keenan *et al.*, 2013), and ADEGENET  
220 v. 2.1.2 (Jombart, 2008; Jombart & Ahmed, 2011). Pairwise  $F_{ST}$ -values were calculated for  
221 clusters inferred from total evidence (see below) using ADEGENET.

222

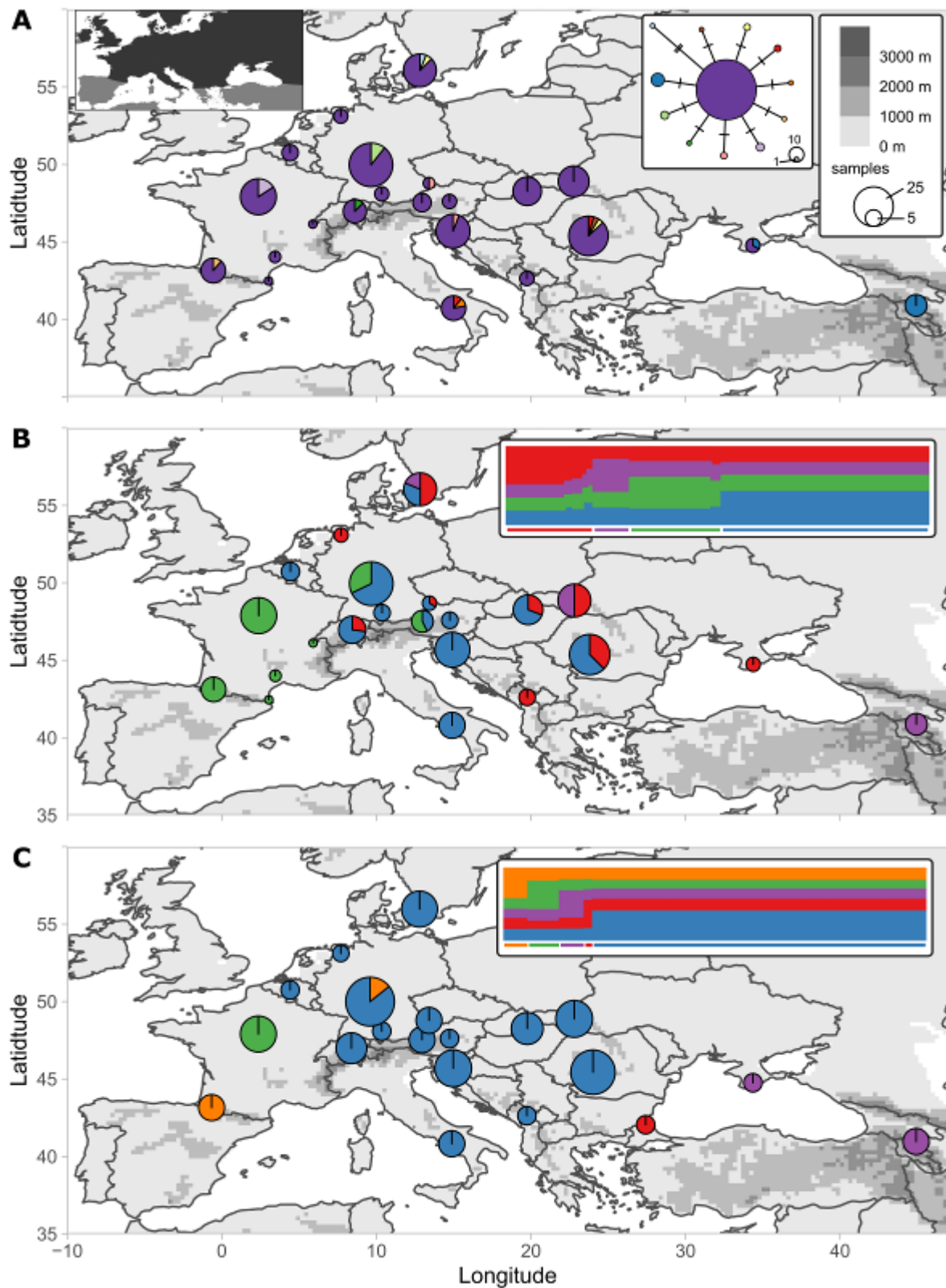
223 Populations of *B. reticulatus* were inferred with GENELAND v. 4.9.2 (Guillot *et al.* 2005b,  
224 2012). GENELAND applies mixture models to infer clusters that are in Hardy-Weinberg  
225 equilibrium with linkage equilibrium between loci. We inferred genetic clusters using the  
226 uncorrelated frequency model based on three datasets: (1) microsatellites, (2) mitochondrial  
227 sequences, and (3) the combination thereof (referred to as total evidence in the following).

228 SNPs were extracted from mitochondrial sequences using ADEGENET. The algorithm considers  
229 geographic coordinates of samples, assuming that populations are spatially separated and  
230 experience little gene flow (spatial model) (Guillot et al. 2005a). A spatial jitter of 0.00001  
231 degree was applied to avoid fixation of samples from one locality in the same cluster. MCMC  
232 chains were run for one million generations (five million for mtDNA), sampling every 1000<sup>th</sup>  
233 generation (5000<sup>th</sup> for mtDNA). Each analysis was repeated three times to ensure stability of  
234 results. Log likelihood and log posterior density trace plots were inspected to ensure  
235 convergence and stationarity of runs and to identify potential outliers that were stuck in local  
236 optima using CODA v. 0.19-3. The maximum number of populations was set to 50, which  
237 roughly corresponds to sampling localities. The maximum rate of the Poisson process was set  
238 to the number of individuals in the respective dataset. The maximum number of nuclei in the  
239 Poisson-Voronoi tessellation was set to two times the number of individuals, which is  
240 suggested for analyses under the spatial model. Null alleles were not filtered. Posterior  
241 samples of each repeat run were separately summarized using the *PostProcessChain*-function  
242 after removing a burn-in of 100,000 generations (400,000 for the total evidence dataset).

243

244 To test for isolation-by-distance, geographic distances were transformed from geographical  
245 coordinates to meters using the RASTER package (Hijmans 2020). Genetic distances were  
246 calculated using ADEGENET (Jombart, 2008; Jombart & Ahmed, 2011). The distances were  
247 plotted against each other for all pairs of sampling locations and complemented by a two-  
248 dimensional density extrapolation to explore potential geographically and genetically isolated  
249 populations. Correlation of the distance matrices was statistically tested by a Mantel test as  
250 implemented in ADE4 (v. 1.7-15; Chessel *et al.*, 2004). Significance was assessed by 10,000  
251 randomizations.

252



253

254

Figure 1: Spatial distribution of (A) 12 mitochondrial haplotypes and haplotype

255

network (*cox1*, *cox2*, and *cob*), (B) four mitochondrial genetic clusters from

256

GENELAND analysis, and (C) five nuclear genetic clusters from GENELAND analyses of

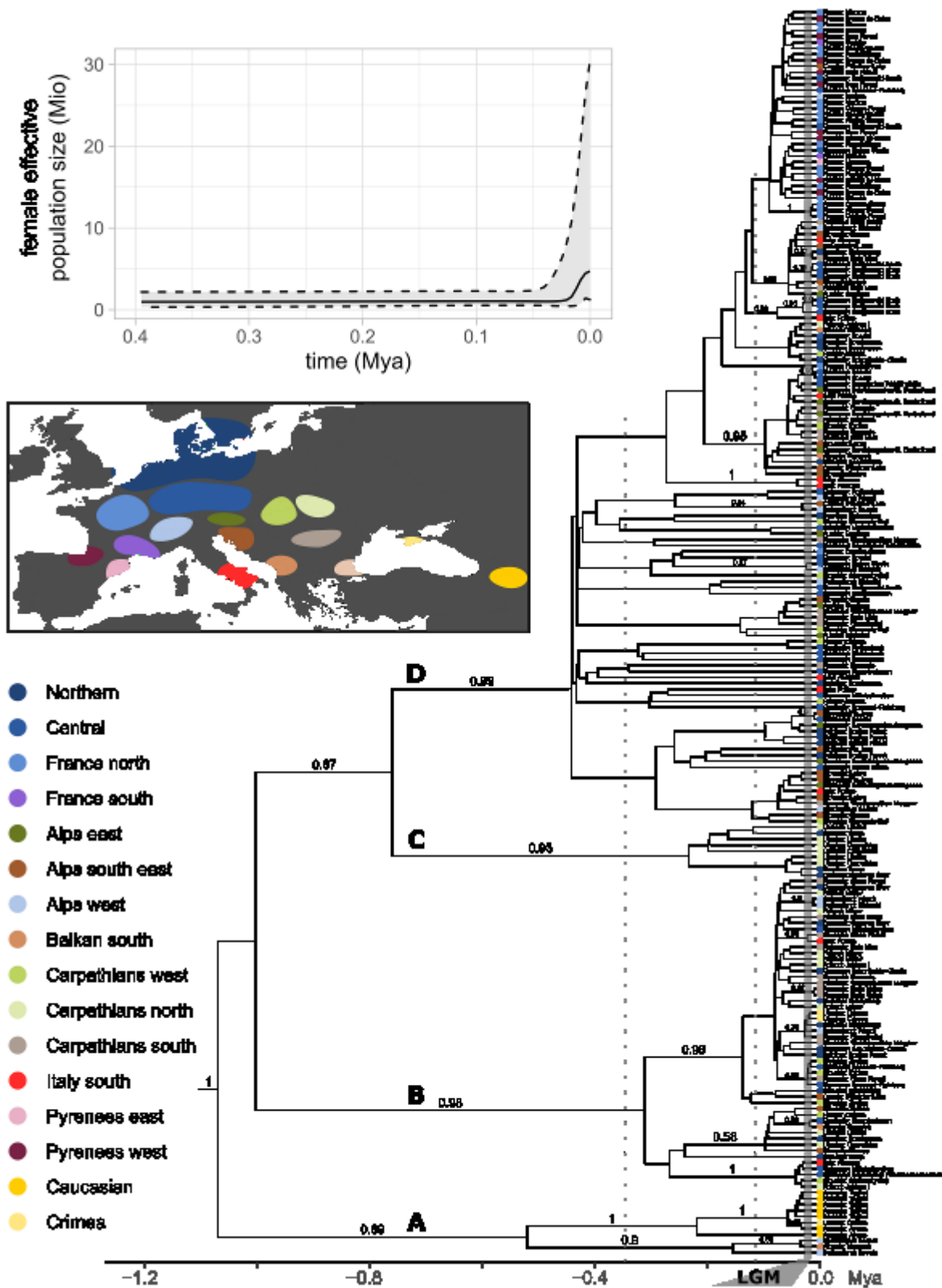
257 polymorphic microsatellites. The size of the pie charts represents the number of  
258 samples; the size of the circles in the haplotype network represents the number of  
259 respective haplotypes. Pie charts may summarize several close by localities. The inset  
260 in (A) shows the approximate distribution of *Bolitophagus reticulatus* in the study area  
261 (own data and [www.gbif.org](http://www.gbif.org)). Insets in (B) and (C) show membership probabilities (y-  
262 axis) of individuals (x-axis) to inferred clusters, which are colour coded for the  
263 respective maps. Coloured bars below the plot indicate assigned group membership.

264

## 265 RESULTS

266 The total concatenated alignment of the three mitochondrial genes consisted of 208  
267 individuals and 1,605 bp (*cox1*: 525 bp, *cox2*: 626 bp, *cob*: 454 bp). Missing data was 1.26%,  
268 2.98%, and 1.19% for *cox1*, *cox2*, and *cob*, respectively. Variation in the mitochondrial genes  
269 was generally low (Appendix Fig. S1). The combined mitochondrial genes differed at twelve  
270 segregating sites (excluding sites with missing or ambiguous data), resulting in twelve  
271 mitochondrial haplotypes (haplotype diversity = 0.24, nucleotide diversity = 0.00024; 167  
272 haplotypes were found using all sites with pairwise deletion of missing and ambiguous data).  
273 One haplotype was noticeably dominant in terms of individual number (in 87% of all  
274 individuals) and distribution range. This haplotype represented the centre of a star-shaped  
275 haplotype network (Fig. 1A, dark violet haplotype). Other, less frequent haplotypes were  
276 regionally restricted with two exceptions that both occurred in the Carpathian Basin (Fig. 1A,  
277 yellow and red haplotypes). GENELAND identified four mitochondrial clusters which  
278 considerably overlapped geographically (Fig. 1B). The Crimean population represented a  
279 combination of haplotypes of the Caucasian and European haplotypes. This pattern was also  
280 discovered with Bayesian and Maximum Likelihood phylogenetic analyses.

281



282

283

284

285

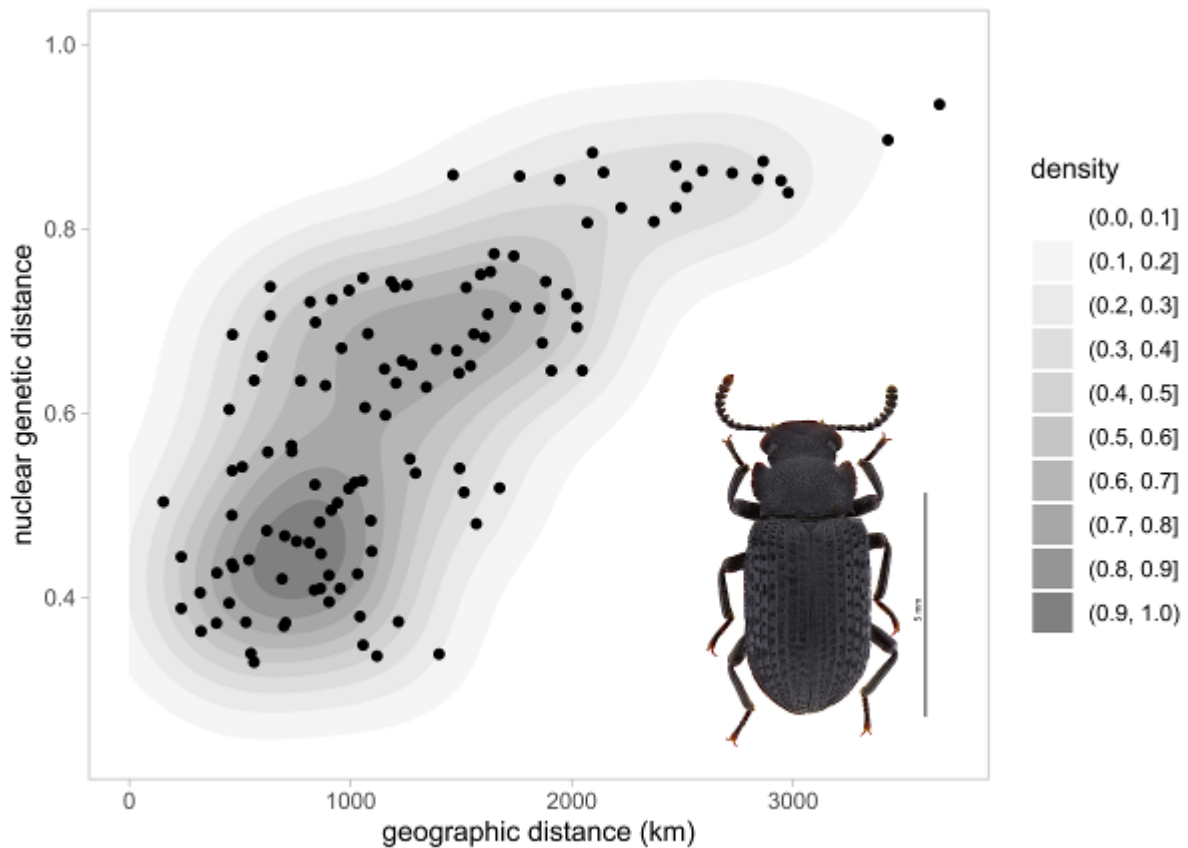
Figure 2: Time calibrated phylogenetic tree from Bayesian analysis of mitochondrial DNA sequences (*cox1*, *cox2*, and *cob*). Vertical dotted lines indicate the onset of the last glacial periods. The vertical grey line marks the last glacial maximum. Colour dots

286 at the trees' tips illustrate geographic origin of the sample. Coloured areas on the map  
287 roughly encircle sampling points of the present study and include refugia of European  
288 and Oriental beech. Upper Inset: Bayesian Skyline plot showing demographic change  
289 in female effective population size over time, assuming a generation time of one year.

290

291 The dated mitochondrial tree from Bayesian inference suggested four major and mostly well  
292 supported clades (Fig. 2 clades A–D). An accumulation of recent diversification events was  
293 detected around 100 kya. Geographic turnover was high, so that specimens from the same  
294 region were rarely restricted to a single clade. The exception were the Caucasus specimens  
295 from Armenia, the easternmost sampling locality, which clustered in one clade together with  
296 one specimen from Crimea. Clades A and B largely included populations from more eastern  
297 locations and showed a connection to the most eastern records of *B. reticulatus* (Ukraine,  
298 Armenia). Those clades also comprised specimens from eastern and northern Europe (Fig. 2).  
299 Clade C was largely restricted to the northern Carpathians, but likewise included specimens  
300 from Denmark and Sweden. Clade D comprised most specimens, originating from all over  
301 Europe except the far eastern localities on Crimea and Armenia. Nearly all populations  
302 sampled across France assembled into one lineage (part of clade D), only interspersed with  
303 three specimens from neighbouring German sites and one from Plitvice Lakes (Croatia).  
304 Posterior supports and crown diversification ages are given in Table 2. The mitochondrial tree  
305 from the maximum likelihood search largely confirmed the genetic clades obtained from  
306 Bayesian analysis, although some topological differences with little support were present  
307 (Appendix Fig. S1, clades A–D). Bayesian Skyline analysis showed a marked increase in  
308 population size since 20 kya, with a recent tendency to reduced growth approximately 5 kya  
309 (Fig. 2).

310



311  
 312 Figure 3: Pairwise geographic and genetic distance between localities illustrate  
 313 isolation by distance. Nuclear genetic distance was inferred from microsatellite data.  
 314 Shades of grey indicate data point density.

315  
 316 Similar to our results obtained from mitochondrial data, global statistics of microsatellite data  
 317 revealed generally low genetic diversity (Appendix Table S3). Observed and expected  
 318 heterozygosity were 0.46 and 0.78, respectively, on average across loci. Mean  $F_{ST}$  was 0.15,  
 319 mean  $G_{ST}$  0.28, mean  $G'_{ST}$  0.64, and mean  $D_{Jost}$  0.50. One nuclear cluster dominated the  
 320 genetic structure based on polymorphic microsatellites (Fig. 1C; blue cluster). However,  
 321 individual cluster composition differed substantially between mitochondrial and nuclear  
 322 inferences. In contrast to results from mitochondrial sequences, nuclear clusters were spatially  
 323 well separated. One exception was a disjunct Pyrenean-German cluster. This is in line with  
 324 low population differentiation indices that were found between three clusters inferred from



325 total evidence (mitochondrial, nuclear, and geography): the  $F_{ST}$  value between a western and  
326 an eastern population was 0.14, while genetic exchange between them and a large central  
327 European cluster seemed to be substantial, resulting in  $F_{ST}$  values  $< 0.05$  (Appendix Figure  
328 S2). Furthermore, we found significant correlation of genetic and geographic distances among  
329 localities based on the Mantel test (expectation from simulation: -0.002, variance: 0.039,  
330 observation: 0.738,  $p < 0.001$ ).

331

## 332 **DISCUSSION**

333 The study of three mitochondrial genes and polymorphic microsatellites allowed us to  
334 reconstruct the postglacial dispersal pathways of *B. reticulatus*. Except for the European-  
335 Caucasian split, which may be due to common isolation of beetle and host tree, we found very  
336 little genetic differentiation. This is most likely explained by genetic depletion in glacial  
337 refugia and rapid postglacial dispersal out of these refugia.

338

### 339 **The European-Caucasian split**

340 The clade restricted to the Caucasus region was clearly distinguishable from the European  
341 clade based on mitochondrial DNA and microsatellite analyses. These genetic signatures  
342 suggest the existence of a refuge area south of the Great Caucasus. This finding goes in line  
343 with previous molecular biogeographic studies on other species where European and  
344 Caucasian populations were included (see e.g., Filipova-Marinova, 1995; Pavlova *et al.*, 2005;  
345 Hansson *et al.*, 2008). Molecular analyses identified a sister species relationship of European  
346 beech (*F. sylvatica*) and Oriental beech (*F. orientalis*) (Renner *et al.*, 2016), which are  
347 distributed in Europe and the Caucasus, respectively ([www.euforgen.org](http://www.euforgen.org); accessed December  
348 [2020](#)). The same isolating forces that caused the intraspecific differentiation in *B. reticulatus*  
349 might have caused speciation in the two beech species. Furthermore, our data indicated the  
350 Crimean region being the contact zone between European populations and the populations of  
351 the Great Caucasus. Previous studies also identified the Crimean region as important contact  
352 zone, e.g. for land snails (Neiber & Hausdorf, 2017).

353

### 354 **Refugia across Central Europe**

355 Infrequent mitochondrial haplotypes occurred regionally restricted, with two exceptions, both  
356 for the Carpathian Basin. This suggests glacial refugia of *B. reticulatus* on the Balkan  
357 Peninsula, and postglacial range expansions across the south-eastern European region, with

358 major areas on the Balkan Peninsula, including the foothills of the Carpathians and areas of  
359 central Europe. This scenario was also supported by phylogenetic inference, and goes in line  
360 with a range of previous studies (reviewed in Schmitt 2007). The postglacial range expansions  
361 from the Balkan Peninsula across major parts of eastern central Europe coincides with the  
362 phylogeography of the European meadow grasshopper *Chorthippus parallelus* (Lunt, Ibrahim,  
363 & Hewitt, 1998), which is name giving to one of the three paradigms stated by Hewitt (Hewitt  
364 1996, 1999, 2000).

365

366 Given the generally high spatial admixture that was evident from mitochondrial DNA in  
367 *B. reticulatus*, it is noteworthy that phylogenetic analyses recovered all but two specimens  
368 from France in one clade, although not well supported (Fig. 2). Likewise, GENELAND  
369 clustered all individuals from France into one cluster when used with mtDNA data and  
370 suggested a connection to central Europe (Fig. 1B). Potential scenarios shaping such pattern  
371 are extra-Mediterranean glacial refugia located at the Massif Central or at the foothills of the  
372 Pyrenees with subsequent postglacial range expansion. This is a frequently observed pattern  
373 in biogeographic studies of organisms of temperate Europe (e.g., Schmitt & Seitz, 2001).  
374 However, the low genetic diversity in France indicates a bottleneck effect during the last  
375 glacial maximum and thus likely small refugia. The multiple extra-Mediterranean glacial  
376 refugia found for *B. reticulatus* (e.g. the Carpathian Basin, Massif Central/Pyrenees) go in line  
377 with findings for various European broadleaf tree species which are used by *F. fomentarius*.  
378 For example, molecular data of the European beech also indicate past refugia at the foothills  
379 of the Pyrenees (Magri 2008). Other studies underline that various tree species of the  
380 European broadleaf forest expanded early after the last glacial maximum northwards, or even  
381 survived in more northern extra-Mediterranean refugia (Chlebicki & Lorenc, 1997; Svenning  
382 *et al.*, 2008; Schmitt & Varga, 2012).

383

384 **Range expansions**

385 The observed genetic structures supported that *B. reticulatus* occurred restrictively in areas  
386 with beech-dominated broadleaf forest providing good conditions for the tinder fungus  
387 (Schwarze, 1994). The tinder fungus and *B. reticulatus* are capable dispersers and likely  
388 exhibit similar post-glacial population expansions. The chronogram in our study indicated an  
389 accumulation of diversification events in *B. reticulatus* with the beginning of the last ice-age  
390 around 100 kya; the median estimate of the onset of population growth was ca. 20 kya, which  
391 coincides with the end of the last glacial maximum. This population growth pattern of *B.*  
392 *reticulatus* inferred from mtDNA suggests range expansions and population increase before  
393 the period of colonization by beech trees, derived from paleontological evidence (Magri *et al.*,  
394 2008). This is an indication that the colonization of the tinder fungus and *B. reticulatus* might  
395 have occurred independently of the beech, and took place much earlier. A plausible scenario  
396 is the expansion together with birch trees, although today in temperate Europe beech is the  
397 main host for the polypore.

398

399 The weak genetic differentiation, alongside high geographic turnover of mtDNA and low  $F_{ST}$   
400 values among regional clusters, as well as the lack of gradual loss of genetic diversity along  
401 potential colonization pathways, allows the inference of the expansion pattern of *B.*  
402 *reticulatus*. While pioneer processes lead to signatures of gradual loss of genetic diversity in  
403 the course of colonization (Ibrahim *et al.* 1996), phalanx-wise colonization results in a lack of  
404 genetic signatures along colonization routes (Hewitt, 2000). The observed lack of genetic  
405 differentiation, in combination with the isolation by distance pattern, approves a phalanx-wise  
406 colonization of Europe and reflects the strong mobility of *B. reticulatus* (Jonsson, 2003).  
407 Similar genetic signatures were also found for the longhorn beetle *Rosalia alpina* (Drag *et al.*,  
408 2018), which inhabits a similar habitat. Our data underline the capability of *B. reticulatus* to

409 rapidly colonize new habitats and the frequent individual exchanges among local populations,  
410 which counteracts potential genetic differentiation.

411 **Data Availability Statement**

412 The mtDNA sequences underlying this article are available in the GenBank Nucleotide  
413 Database at [www.ncbi.nlm.nih.gov/genbank/](http://www.ncbi.nlm.nih.gov/genbank/), and can be accessed with the accession  
414 numbers MH383529–MH383770 for *cob*, MH383771–MH384020 for *cox1*, and MH384021–  
415 MH384258 for *cox2*. Sequence alignments and phylogenetic trees are available in TreeBase at  
416 <http://purl.org/phylo/treebase/phylows/study/TB2:S27736>. Microsatellite data are available in  
417 the online supplementary material (Appendix Table S2).

418

419 **Supporting Information**

420 Additional Supporting Information may be found in the online version of this article at the  
421 publisher's web-site:

422

423 Table S1: Sampling sites and genetic diversity measures.

424

425 Table S2: GenBank Accession numbers for mtDNA sequences and microsatellite data.

426

427 Table S3: Global statistics of microsatellite data.

428

429 Figure S1. Mitochondrial tree from maximum likelihood analysis.

430

431 Figure S2. Spatial distribution of three clusters inferred by GENELAND based on total  
432 evidence.

433

434 **Acknowledgements**

435 We highly appreciate valuable comments by Thomas Schmitt on an earlier version of this  
436 article. We thank Sarah Sturm, Jose Angel Rangel Lopez and Yasemin Guenay for laboratory  
437 work. Simon Thorn, Radosław Gil, and Barbara Winter kindly contributed further samples.  
438 This project was financed by the Bayerisches Staatsministerium für Ernährung,  
439 Landwirtschaft und Forst (Grant L55) and the Technical University Munich. W.U. was  
440 supported by an internal NCU IDUB grant. We thank the LWF and the Bavarian State  
441 Forestry BaySF for fruitful collaboration. In particular, we want to thank Ulrich Mergner,  
442 Nadja Simons for their help in the field. We are grateful for three valuable reviews of our  
443 manuscript.

444

445 **References**

- 446 **Becker RA, Wilks AR (Original S code), Brownrigg R, Minka TP, Deckmyn A (R**  
447 **version). 2018.** maps: Draw Geographical Maps. R package version 3.3.0.  
448 <https://CRAN.R-project.org/package=maps>
- 449 **Bouget C, Brustel H, Noblecourt T, Zagatti P. 2019.** *Les Coléoptères saproxyliques de*  
450 *France – Catalogue écologique illustré*, Muséum national d'Histoire naturelle, Paris,  
451 744p. (Patrimoines naturels; 79).
- 452 **Boukaert R, Heled J, Kühnert D, Vaughan T, Wu CH, Xie D, Suchard MA, Rambaut A**  
453 **& Drummond AJ. 2014.** BEAST 2: A Software Platform for Bayesian Evolutionary  
454 Analysis. *PLOS computational biology* **10**: 1–6.
- 455 **Brunet J, Fritz Ö & Richnau G. 2010.** Biodiversity in European beech forests – a review  
456 with recommendations for sustainable forest management. *Ecological Bulletin* **55**: 77–  
457 94.
- 458 **Chessel D, Dufour A & Thioulouse J. 2004.** The ade4 Package – I: One-Table Methods. *R*  
459 *News* **4**: 5–10.
- 460 **Chlebicki A & Lorenc MW. 1997.** Subfossil Fomes fomentarius from a Holocene fluvial  
461 deposit in Poland. *The Holocene* **7**: 101–103.
- 462 **Drag L, Hauck D, Bérces S, Michalcewicz J, Jelaska LS, Aurenhammer S, Cizek L.**  
463 **2015.** Genetic differentiation of populations of the threatened saproxylic beetle  
464 Rosalia Longicorn, *Rosalia alpina* (Coleoptera: Cerambycidae) in Central and South-  
465 east Europe. *Biological Journal of the Linnean Society* **116**: 911–925.
- 466 **Drag L, Hauck D, Pokluda P, Zimmermann K, Cizek L. 2011.** Demography and dispersal  
467 ability of a threatened saproxylic beetle: A mark-recapture study of the Rosalia  
468 longicorn (*Rosalia alpina*). *PLoS One* **6**: e21345.
- 469 **Drag L, Hauck D, Rican O, Schmitt T, Shovkoon DF, Godunko RJ, Curletti G, Cizek L.**  
470 **2018.** Phylogeography of the endangered saproxylic beetle Rosalia longicorn *Rosalia*  
471 *alpina* (Coleoptera, Cerambycidae), corresponds with its main host, the European  
472 beech (*Fagus sylvatica*, Fagaceae). *Journal of Biogeography* **45**: 2631–2644.
- 473 **Drummond AJ, Rambaut A, Shapiro B & Pybus OG. 2005.** Bayesian Coalescent  
474 Inference of Past Population Dynamics from Molecular Sequences. *Molecular Biology*  
475 *and Evolution* **22**: 1185–1192.
- 476 **Edgar RC. 2004a.** MUSCLE: multiple sequence alignment with high accuracy and high  
477 throughput. *Nucleic Acids Research* **32**: 1792–1797.



- 478 **Edgar RC. 2004b.** MUSCLE: a multiple sequence alignment method with reduced time and  
479 space complexity. *BMC Bioinformatics* **5**: 113.
- 480 **Filipova-Marinova M. 1995.** Late Quaternary history of the Genus *Fagus* in Bulgaria. In  
481 Bozilova E & Tonkov S (eds). *Advances in Holocene Palaeoecology in Bulgaria*.  
482 Pensoft Publishers.
- 483 **Friess N, Müller JC, Abrego N, Aramendi P, Bässler C, Bouget C, Brin A, Bussler H,**  
484 **Georgiev K, Gil R, Gossner MM, Heilmann-Clausen J, Isaacson G, Krištin A,**  
485 **Lachat T, Larrieu L, Los S, Magnanou E, Maringer A, Mergner U, Mikolas M,**  
486 **Opgenoorth L, Schmidl J, Svoboda M, Thorn S, Vrezec A, Vanderkhoven K,**  
487 **Winter B, Wagner T, Zapponi L, Brandl R & Seibold S. 2019.** The species-rich  
488 arthropod communities in fungal fruitbodies are weakly structured by climate and  
489 biogeography across European beech forests. *Diversity and Distributions* **25**: 783-796.
- 490 **Giesecke T, Brewer S, Finsinger W, Leydet M & Bradshaw RHW. 2017.** Patterns and  
491 dynamics of European vegetation change over the last 15,000 years. *Journal of*  
492 *Biogeography* **44**: 1441–1456.
- 493 **Guillot G, Estoup A, Mortier F, Cosson JF. 2005a.** A spatial statistical model for landscape  
494 genetics. *Genetics* **170**: 1261–1280.
- 495 **Guillot G, Mortier F, Estoup A. 2005b.** Geneland: A program for landscape genetics.  
496 *Molecular Ecology Notes* **5**: 712–715.
- 497 **Guillot G, Renaud S, Ledevin R, Michaux J, Claude J. 2012.** A Unifying Model for the  
498 Analysis of Phenotypic, Genetic and Geographic Data. *Systematic Biology*, **61**: 897–  
499 911.
- 500 **Habel JC, Mulwa RK, Gassert F, Rödder D, Ulrich W, Borghesio L, Husemann M &**  
501 **Lens L. 2014.** Population signatures of large-scale, long-term disjunction and small-  
502 scale, short-term habitat fragmentation in an Afrotropical forest bird. *Heredity* **113**:  
503 205–214.
- 504 **Hansson B, Hasselquist D, Tarka M, Zehndjiev P & Bensch S. 2008.** Postglacial  
505 Colonisation Patterns and the Role of Isolation and Expansion in Driving  
506 Diversification in a Passerine Bird. *PLOS ONE* **3**: e2794.
- 507 **Hewitt GM. 1996.** Some genetic consequences of ice ages, and their role in divergence and  
508 speciation. *Biological Journal of the Linnean Society* **58**, 247–276.
- 509 **Hewitt GM. 1999.** Post-glacial recolonization of European biota. *Biological Journal of the*  
510 *Linnean Society* **68**: 87–112.
- 511 **Hewitt GM. 2000.** The genetic legacy of the Quaternary ice ages. *Nature* **405**: 907–913.

- 512 **Hijmans RJ. 2020.** raster: Geographic Data Analysis and Modelling. R package version 3.1-  
513 5. <https://CRAN.R-project.org/package=raster>
- 514 **Hoang DT, Chernomor O, von Haeseler A, Minh BQ, Vinh LS. 2018.** UFBoot2:  
515 Improving the Ultrafast Bootstrap Approximation. *Molecular Biology and Evolution*  
516 **35:** 518–522.
- 517 **Ibrahim KM, Nichols RA, Hewitt GM. 1996.** Spatial patterns of genetic variation generated  
518 by different forms of dispersal during range expansion. *Heredity* **77:** 282–291.
- 519 **Iwan D, Löbl I, Bouchard P, Bousquet Y, Kamiński M, Merkl O, Ando K & Schawaller**  
520 **W. 2020.** Family Tenebrionidae Latreille, 1802. In: Iwan D, Löbl I, eds. *Catalogue of*  
521 *Palearctic Coleoptera, Volume 5, Tenebrionoidea*. Revised and updated second  
522 edition. Leiden: Brill NV, 969 pp.
- 523 **Jiménez-Alfaro B, Girardello M, Chytrý M, Svenning JC, Willner W, Gégout JC,**  
524 **Agrillo E, Campos JA, Jandt U, Kački Z, Šilc U, Slezák M, Tichý L, Tsiripidis I,**  
525 **Turtureanu PD, Ujházyová M & Wohlgemuth T. 2018.** History and environment  
526 shape species pools and community diversity in European beech forests. *Nature*  
527 *Ecology & Evolution* **2:** 483–490.
- 528 **Jombart T. 2008.** adegenet: a R package for the multivariate analysis of genetic markers.  
529 *Bioinformatics* **24:** 1403-1405.
- 530 **Jombart T, Ahmed I. 2011.** adegenet 1.3-1: new tools for the analysis of genome-wide SNP  
531 data. *Bioinformatics*.
- 532 **Jonsson M. 2003.** Colonisation ability of the threatened tenebrionid beetle *Oplocephala*  
533 *haemorrhoidalis* and its common relative *Bolitophagus reticulatus*. *Ecological*  
534 *Entomology* **28:** 159–167.
- 535 **Jonsell M, Schroeder M, Larsson T. 2003.** The saproxylic beetle *Bolitophagus reticulatus*:  
536 its frequency in managed forests, attraction to volatiles and flight period. *Ecography*  
537 **26:** 421 – 428.
- 538 **Jonsson M, Johannesen J & Seitz A. 2003.** Comparative genetic structure of the threatened  
539 tenebrionid beetle *Oplocephala haemorrhoidalis* and its common relative  
540 *Bolitophagus reticulatus*. *Journal of Insect Conservation* **7:** 111–124.
- 541 **Kalyaanamoorthy S, Minh BQ, Wong TKF, von Haeseler A, Jermini LS. 2017.**  
542 ModelFinder: fast model selection for accurate phylogenetic estimates. *Nature*  
543 *Methods* **14:** 587–589.
- 544 **Kamvar ZN, Tabima JF, Grünwald NJ. 2014.** Poppr: an R package for genetic analysis of  
545 populations with clonal, partially clonal, and/or sexual reproduction. *PeerJ* **2:** e281.

- 546 **Kamvar ZN, Brooks JC and Grünwald NJ. 2015.** Novel R tools for analysis of genome-  
547 wide population genetic data with emphasis on clonality. *Frontiers in Genetics* **6**: 208.
- 548 **Keenan K, McGinnity P, Cross TF, Crozier WW & Prodöhl PA. 2013.** diveRsiTy: An R  
549 package for the estimation of population genetics parameters and their associated  
550 errors. *Methods in Ecology and Evolution* **4**: 782–788.
- 551 **Kergoat GJ, Soldati L, Clamens AL, Jourdan H, Jabbour-Zahab R, Genson G,**  
552 **Bouchard P & Condamine FL. 2014.** Higher level molecular phylogeny of darkling  
553 beetles (Coleoptera: Tenebrionidae). *Systematic Entomology* **39**: 486–499.
- 554 **Knutsen H, Rukke BA, Jorde PE & Ims RA. 2000.** Genetic differentiation among  
555 populations of the beetle *Bolitophagus reticulatus* (Coleoptera: Tenebrionidae) in a  
556 fragmented and a continuous landscape. *Heredity* **84**: 667–676.
- 557 **Lunt DH, Ibrahim KM & Hewitt GM. 1998.** mtDNA phylogeography and postglacial  
558 patterns of subdivision in the meadow grasshopper *Chorthippus parallelus*. *Heredity*  
559 **80**: 633–641.
- 560 **Magri D, Vendramin GG, Comps B, Dupanloup I, Geburek T, Gomory D, Latalowa M,**  
561 **Litt T, Paule L, Roure JM, Tantau I, van der Knaap WO, Petit RJ & de Beaulieu**  
562 **JL. 2006.** A new scenario for the Quaternary history of European beech populations:  
563 palaeobotanical evidence and genetic consequences. *New Phytologist* **171**: 199–221.
- 564 **Magri D. 2008.** Patterns of post-glacial spread and the extent of glacial refugia of European  
565 beech (*Fagus sylvatica*). *Journal of Biogeography* **35**: 450–463.
- 566 **Midtgaard F, Rukke BA & Sverdrup-Thygeson A. 1998.** Habitat use of the fungivorous  
567 beetle *Bolitophagus reticulatus* (Coleoptera: Tenebrionidae): Effects of basidiocarp  
568 size, humidity and competitors. *European Journal of Entomology* **95**: 559–570.
- 569 **Minh BQ, Schmidt HA, Chernomor O, Schrempf D, Woodhams MD, von Haeseler A,**  
570 **Lanfear R. 2020.** IQ-TREE 2: New models and efficient methods for phylogenetic  
571 inference in the genomic era. *Molecular Biology and Evolution*
- 572 **Müller J, Brunet J, Brin A, Bouget C, Brustel H, Bussler H, Förster B, Isacson G,**  
573 **Köhler F, Lachat T & Gossner MM. 2013.** Implications from large-scale spatial  
574 diversity patterns of saproxylic beetles for the conservation of European Beech forests.  
575 *Insect Conservation and Diversity* **6**: 162–169.
- 576 **Neiber MT & Hausdorf B. 2015.** Phylogeography of the land snail genus *Circassina*  
577 (Gastropoda: Hygromiidae) implies multiple Pleistocene refugia in the western  
578 Caucasus region. *Molecular Phylogenetics and Evolution* **93**: 129–142.

- 579 **Neiber MT & Hausdorf B. 2017.** Molecular phylogeny and biogeography of the land snail  
580 genus *Monacha* (Gastropoda, Hygromiidae). *Zoologica Scripta* **46**: 308–321.
- 581 **Nilsson T. 1997.** Survival and habitat preferences of adult *Bolitophagus reticulatus*.  
582 *Ecological Entomology* **22**: 82–89.
- 583 **Papadopoulou A, Anastasiou I, Vogler AP 2010.** Revisiting the insect mitochondrial  
584 molecular clock: The mid-aegean trench calibration. *Molecular Biology and Evolution*  
585 **27**: 1659–1672.
- 586 **Paradis E. 2010.** pegas: an R package for population genetics with an integrated-modular  
587 approach. *Bioinformatics* **26**: 419–420.
- 588 **Pavlova A, Zink RM, Rohwer S, Koblik EA, Red'kin YA, Fadeev IV & Nesterov EV.**  
589 **2005.** Mitochondrial DNA and plumage evolution in the white wagtail *Motacilla alba*.  
590 *Journal of Avian Biology* **36**: 322–336.
- 591 **Pons JM, Olliso G, Cruaud C & Fuchs J. 2011.** Phylogeography of the Eurasian green  
592 woodpecker (*Picus viridis*). *Journal of Biogeography* **38**: 311–325.
- 593 **Pott R. 2000.** Die Entwicklung der europäischen Buchenwälder in der Nacheiszeit.  
594 *Rundgespräche der Kommission für Ökologie*, **18**, 49–75.
- 595 **R Core Team. 2019.** R: A language and environment for statistical computing. R Foundation  
596 for statistical Computing, Vienna, Austria. URL <https://www.R-project.org/>.
- 597 **Rambaut A, Drummond AJ, Xie D, Baele G, Suchard MA. 2018.** Posterior Summarization  
598 in Bayesian Phylogenetics Using Tracer 1.7. *Systematic Biology* **67**: 901–904.
- 599 **Rangel López JÁ, Husemann M, Schmitt T, Kramp K & Habel JC. 2018.** Mountain  
600 barriers and trans-Saharan connections shape the genetic structure of *Pimelia* darkling  
601 beetles (Coleoptera: Tenebrionidae). *Biological Journal of the Linnean Society* **124**:  
602 547–556.
- 603 **Renner SS, Grimm GW, Kapli P, Denk T. 2016.** Species relationships and divergence  
604 times in beeches: new insights from the inclusion of 53 young and old fossils in a  
605 birth–death clock model. *Philosophical Transactions of the Royal Society B*: **371**:  
606 20150135.
- 607 **RStudio Team. 2018.** RStudio: Integrated Development for R. RStudio, Inc., Boston, MA  
608 URL <http://www.rstudio.com/>.
- 609 **Rukke BA. 2000.** Effects of habitat fragmentation: increased isolation and reduced habitat  
610 size reduces the incidence of dead wood fungi beetles in a fragmented forest  
611 landscape. *Ecography* **23**: 492–502.

- 612 **Saltré F, Saint-Amant R, Gritti ES, Brewer S, Gaucherel C, Davis BAS & Chuine I.**  
613 **2013.** Climate or migration: what limited European beech post-glacial colonization?  
614 *Global Ecology and Biogeography* **22**: 1217–1227.
- 615 **Schmitt T. 2007.** Molecular biogeography of Europe: Pleistocene cycles and postglacial  
616 trends. *Frontiers in Zoology* **4**: 11.
- 617 **Schmitt T, Varga Z. 2012.** Extra-Mediterranean refugia: The rule and not the exception?  
618 *Frontiers in Zoology* **9**: 22.
- 619 **Schwarze F. 1994.** Wood rotting fungi: *Fomes fomentarius* (L.: Fr.) Fr.: Hoof or tinder  
620 fungus. *Mycologist* **8**: 32–34.
- 621 **Stauffer C, Lakatos F & Hewitt GM. 1999.** Phylogeography and postglacial colonization  
622 routes of *Ips typographus* L. (Coleoptera, Scolytidae). *Molecular Ecology* **8**: 763–773.
- 623 **Svenning JC, Normand S & Kageyama M. 2008.** Glacial refugia of temperate trees in  
624 Europe: insights from species distribution modelling. *Journal of Ecology* **96**: 1117–  
625 1127.
- 626 **Tarkhnishvili D, Gavashelishvili A & Mumladze L. 2012.** Palaeoclimatic models help to  
627 understand current distribution of Caucasian forest species. *Biological Journal of the*  
628 *Linnean Society* **105**: 231–248.
- 629 **Wickham H. 2016.** ggplot2: Elegant Graphics for Data Analysis. Springer-Verlag New York.
- 630 **Zytynska SE, Doerfler I, Gossner MM, Sturm S, Weisser WW, Müller J. 2018.** Minimal  
631 effects on genetic structuring of a fungus-dwelling saproxylic beetle after  
632 recolonisation of a restored forest. *Journal of Applied Ecology* **55**: 2933– 2943.  
633

634 **Figures**

635 Figure 1: Spatial distribution of (A) 12 mitochondrial haplotypes and haplotype network  
636 (*cox1*, *cox2*, and *cob*), (B) four mitochondrial genetic clusters from GENELAND analysis, and  
637 (C) five nuclear genetic clusters from GENELAND analyses of polymorphic microsatellites.  
638 The size of the pie charts represents the number of samples; the size of the circles in the  
639 haplotype network represents the number of respective haplotypes. Pie charts may summarize  
640 several close by localities. The inset in (A) shows the approximate distribution of  
641 *Bolitophagus reticulatus* in the study area (own data and [www.gbif.org](http://www.gbif.org)). Insets in (B) and (C)  
642 show membership probabilities (y-axis) of individuals (x-axis) to inferred clusters, which are  
643 colour coded for the respective maps. Coloured bars below the plot indicate assigned group  
644 membership.

645

646 Figure 2: Time calibrated phylogenetic tree from Bayesian analysis of mitochondrial DNA  
647 sequences (*cox1*, *cox2*, and *cob*). Vertical dotted lines indicate the onset of the last glacial  
648 periods. The vertical grey line marks the last glacial maximum. Colour dots at the trees' tips  
649 illustrate geographic origin of the sample. Coloured areas on the map roughly encircle  
650 sampling points of the present study and include refugia of European and Oriental beech.  
651 Upper Inset: Bayesian Skyline plot showing demographic change in female effective  
652 population size over time, assuming a generation time of one year.

653

654 Figure 3: Pairwise geographic and genetic distance between localities illustrate isolation by  
655 distance. Nuclear genetic distance was inferred from microsatellite data. Shades of grey  
656 indicate data point density.

657

658

659 **Tables**

660 Table 1: Investigated regions and genetic diversities obtained for all populations analysed.

661 Given are the coordinates in decimal format (WGS84), the number of mitochondrial DNA

662 samples  $n_{mt}$ , haplotypes  $HT$ , nuclear DNA samples  $n_n$ , alleles  $A$ , and allele combinations, as

663 well as observed and expected heterozygosity,  $H_o$ , and  $H_e$  respectively.

664

<i>region</i>	$n_{mt}$	$HT$	$n_n$	$A$	<i>Comb.</i>	$H_o$	$H_e$
Alps east	8	1	15	95	106	0.35	0.61
Alps south-east	17	2	20	146	195	0.50	0.77
Alps west	9	2	14	138	150	0.48	0.75
Balkan east	na	na	5	47	50	0.48	0.48
Balkan south	3	1	5	86	76	0.63	0.70
Carpathians north	14	1	20	129	175	0.48	0.70
Carpathians south	23	4	29	156	223	0.46	0.72
Carpathians west	12	1	15	97	122	0.44	0.65
Caucasian	7	1	10	38	43	0.16	0.24
Central	33	3	50	177	299	0.51	0.74
Crimea	3	2	5	49	51	0.39	0.48
France north	19	2	19	93	142	0.50	0.62
France south	2	1	na	na	na	na	na
Italy south	9	3	10	102	117	0.51	0.72
Northern	23	3	28	149	228	0.45	0.75
Pyrenees east	1	1	na	na	na	na	na
Pyrenees west	9	2	10	71	82	0.42	0.53

665

666

667 Table 2: Crown ages of major lineages from Bayesian divergence dating (compare Fig. 2).

Node	Posterior clade support	Median age (kya)	Mean age (kya)	95 % HPD interval (kya)
Root	1.00	971.8	1070.5	398.8 – 1960.6
A	0.89	400.3	456.3	107.1 – 928.7
B	0.98	279.2	308.2	102.3 – 582.2
C + D	0.67	585.7	644.8	234.5 – 1181.8
C	0.93	174.5	216.1	24.2 – 515.5
D	0.99	389.2	434.0	153.8 – 818.5

668